

# RISK DEPENDENT SEISMIC DESIGN

Mircea Grigoriu

## SYNOPSIS

A simple method for seismic design is developed based on the mean failure rate, or the mean crossing rate of the response vector out of the region of safe behaviour for a structure. The components of the response vector are earthquake effects at the critical points of the structure. A knowledge of the spectral density of the ground acceleration, the target mean failure rate, and the modal parameters of the structure is needed for application of the method. Resultant structures are anticipated to fail at a mean rate smaller than the target value. Results reported for a shear frame and an asymmetrical structure demonstrate that the actual and the target mean failure rates are nearly equal for many situations of practical interest.

## RESUME

Une méthode simple de calcul antisismique est développée d'après le taux de rupture moyen ou le taux de croisement moyen sur le vecteur de réponse hors de la zone de comportement sécuritaire de la structure. Les éléments du vecteur de réponse sont des effets sismiques aux points critiques de la structure. Une connaissance de la densité du spectre, de l'accélération au sol, du taux de rupture moyen cible et des propriétés modales de la structure s'avère nécessaire pour l'application de la méthode. On prévoit que les structures analysées se ruptureront à un taux moyen moins élevé que la valeur cible. Les résultats rapportés pour l'ossature soumise au cisaillement et pour une structure asymétrique démontrent que les taux de ruptures réels et les taux de ruptures moyens cibles sont presque égaux pour toute situation d'intérêt pratique.

M. Grigoriu obtained his Ph.D. from the Massachusetts Institute of Technology, Cambridge, in 1976. He is currently a Lead Engineer in the Structural Mechanics Department of Acres Consulting Services Limited.

## INTRODUCTION

Seismic design of many structures, such as tall buildings or equipment and piping systems of nuclear plants, is based on the requirement that the maximum response at the critical points does not exceed an allowable value. The maximum response is obtained in general by combining extreme responses recorded in various modes of vibration excited by the design earthquake, where modal response maxima can be obtained from the response spectrum. The absolute or algebraic sum and the square root of the sum of the squares of the largest modal responses are combination rules currently used in practice. It is assumed typically that the structure is as safe as the critical points. Findings of this paper show that the assumption can be unconservative, when complex structures are involved. In addition, the response spectrum method lacks control over reliability.

A major purpose of this paper is the development of a method for seismic design of structures of prescribed reliability when the ground acceleration is random. This risk dependent method is based on the random vibration theory and results reported in (16). A structure is deemed safe if the random, time-dependent response vector never leaves a region of safe behaviour during the reference period; the safety of a structure is inferred from that of the critical points considered simultaneously. The components of the response vector are earthquake effects at the critical points. The safe region and the response vector depend on the probability law of the ground acceleration, and the modal parameters of the structure. The target reliability controls the size of the safe region.

Safety estimates are based on the mean failure rate, or the mean rate at which the response vector crosses out of the safe region. The dependence of the mean failure rate and reliability on the correlation between responses at the critical points is investigated in the next section. Approximations for the mean failure rate and useful results regarding the correlation between modal coordinates are also reported. Application of the risk dependent method is demonstrated for structures with widely and closely spaced modal frequencies. For comparison, the current design approach is extended to account for the uncertainty in the ground acceleration. Results reported correspond to a stationary Gaussian ground acceleration with constant spectral density.

## STRUCTURES SUBJECTED TO BASE RANDOM MOTION

Structural systems having a finite number,  $n$ , of degrees-of-freedom and classical modes of vibration are considered only. It is assumed that the ground acceleration,  $A(t)$ , is a weakly stationary random process with a mean of zero and that the structure is in steady-state motion.

The coordinate,  $D_j(t)$ , of the  $j$ 'th mode is also a stationary process in the wide sense which satisfies the differential equation:

$$D_j''(t) + 2\beta_j\omega_j D_j'(t) + \omega_j^2 D_j(t) = -\Gamma_j A(t) \quad (1)$$

The dots denote the derivative with respect to time and  $\omega_j$ ,  $\beta_j$ , and  $\Gamma_j$  are the frequency, the coefficient of damping or damping ratio, and the participation factor, respectively, for the  $j$ 'th mode.

Correlation between Modal Coordinates

The covariance matrix of the vector  $\underline{X}^T(t) = \{D_1(t), D_1'(t), D_2(t), D_2'(t)\}$  is evaluated in Appendix I based on the theory of linear systems for an uncorrelated ground acceleration,  $A(t)$ , with one-sided spectral intensity  $G_0$ . The approach can be used also when  $A(t)$  is correlated. In this case, the ground acceleration,  $A(t)$ , and its derivatives can be modeled by a linear system with state vector  $\underline{A}^T(t) = \{A(t), A'(t), \dots\}$  driven by white noise. The covariance matrix of  $\underline{X}(t)$  can be found also from Eq. 21 applied for the augmented system with state vector  $\{\underline{X}^T(t), \underline{A}^T(t)\}$ .

Shown in Fig. 1 is the variation of the correlation coefficients,  $\rho_{13}$  and  $\rho_{24}$ , for the modal coordinates  $\{D_i(t), D_j(t)\}$  and their derivatives  $\{D_i'(t), D_j'(t)\}$ , respectively, with the ratio,  $\lambda = \omega_i/\omega_j$ , of modal frequencies when  $\beta = \beta_i = \beta_j$ . The correlation coefficients  $\rho_{13}$  and  $\rho_{24}$  are equal when the modes have the same damping ratio and increase with  $\beta$ , as shown also by Eq. 23. They are approximately 0.07, 0.29, and 0.61 for  $\beta = 0.02, 0.05,$  and  $0.1$ , respectively, when  $\lambda = 0.8$ . The modal coordinates are nearly unrelated for many cases of practical interest and are perfectly correlated as  $\omega_i = \omega_j$ .

Correlation coefficients between modal coordinates having different damping ratios are shown in Fig. 2. The correlation coefficients  $\rho_{13}$  and  $\rho_{24}$  vary with  $\mu = \beta_i/\beta_j$  monotonically, for given  $\beta_j$  and  $\lambda$ . They are nearly equal for the cases considered. Modes having different damping ratios are never perfectly correlated. The largest value of  $\rho_{13}$  and  $\rho_{24}$  is found when the modal frequencies are nearly equal. The dependence of the correlation coefficients  $\rho_{13}$  and  $\rho_{24}$  on  $\mu = \beta_i/\beta_j$  for  $\omega_i = \omega_j$  is demonstrated in Fig. 3. From Eq. 23,  $\rho_{13} = \rho_{24}$  when  $\lambda = 1.0$ .

Results in Figs. 1 to 3 show also that the coordinates of the first few modes for symmetrical buildings of shear or flexural beam

type are nearly unrelated for common damping ratios because  $\omega_2/\omega_1 = 3.0$ ;  $\omega_3/\omega_2 = 1.67$ ;  $\omega_3/\omega_1 = 5.01$  or  $\omega_2/\omega_1 = 6.27$ ;  $\omega_3/\omega_2 = 2.80$ ;

$\omega_3/\omega_1 = 17.56$ , respectively. However, the coordinates of translational and torsional modes for asymmetrical structures can be strongly related for many practical situations.

Note also that the correlation level between  $\{D_j(t)\}$  controls the accuracy of modal combination rules, such as the absolute (ABS) or algebraic (ALS) sum and the square root of the sum of the square (RSS) of the largest modal responses. For example, the RSS rule yields satisfactory results when the modal coordinates are weakly related (11, 14). On the other hand, the ABS or ALS procedures are accurate when the modal responses are in or completely out of phase, respectively. The latter conditions are satisfied with approximation for strongly related modal coordinates. The rules considered can be inaccurate when the coordinates of the significant modes have very different correlation levels. In this case, strongly related modal responses can be combined according to the ABS or ALS rules. The RSS rule can be used then to combine remaining modal responses with effects obtained in the first step.

These considerations of accuracy of the modal combination rules do not apply to complex structures in general, because the critical points can be much safer than the structure in these cases (3, 7). To account for this effect, building codes of many countries postulate larger design levels for complex structures, for example. The approach is arbitrary, however.

#### Estimation of Reliability

Consider a  $n$  degree-of-freedom structure subjected to a Gaussian ground acceleration,  $A(t)$ , for a period,  $\tau$ . The behaviour of the structure is assumed linear so as the load effect at the  $k$ 'th critical point is,

$$Y_k(t) = \sum_{j=1}^n c_{kj} D_j(t) \quad (k = 1, 2, \dots, m) \quad (2)$$

The number,  $m$ , of critical points may not be equal to  $n$ . The coefficients,  $\{c_{kj}\}$ , are linear functions of the modal shapes. They can depend also on parameters such as structural stiffnesses, geometry, or sectional characteristics when  $\{Y_k(t)\}$  denote stresses.

The structure is safe if the following conditions are satisfied during  $\tau$ ,

$$-d_k' \leq Y_k(t) \leq d_k'' \quad (k = 1, 2, \dots, m) \quad (3)$$

where  $d_k'$  and  $d_k''$  are allowable values depending on the load effect and the structural elements involved. The safety condition can be expressed also in terms of the response vector,  $\underline{Y}^T(t) = \{Y_1(t), Y_2(t), \dots, Y_m(t)\}$ , in which case the reliability is the probability that  $\underline{Y}(t)$  never leaves the safe region,  $D$ , during  $\tau$ ,

$$P_s(\tau) = P(\underline{Y}(t) \in D, t \in (0, \tau)) \quad (4)$$



where  $P(B)$  is the probability of event  $B$ . From Eq. 3, the safe region is a rectangle in the  $m$ -dimensional space. Shown in Figs. 4 and 6 are rectangular safe regions yielded by Eq. 3 for  $m=2$ .

The reliability is (2,4,10,16),

$$P_S(\tau) = P(\underline{Y}(0) \in D) \exp(-\nu\tau) \quad (5)$$

where  $\nu$  is the mean failure rate, or the mean rate at which  $\underline{Y}(t)$  crosses the boundary,  $\partial D$ , of the safe region,  $D$ , from inside, and  $P(\underline{Y}(0) \in D)$  is the instantaneous reliability at  $t=0$ . The result is based on the assumption that the crossings of  $\underline{Y}(t)$  follow a homogeneous Poisson process with mean rate of  $\nu$ . This assumption is accurate when  $\underline{Y}(t)$  belongs to  $D$  with large probability, at any time (4).

Evaluation of the mean failure rate,  $\nu$ , may be numerically prohibitive. From (2),

$$\nu = \int_{\partial D} d\underline{y} \int_0^{\infty} dy'_n y'_n f_{\underline{Y}, Y'_n}(\underline{y}, y'_n) \quad (6)$$

where  $f_{\underline{Y}, Y'_n}$  is the joint density of  $\underline{Y}(t)$  and  $Y'_n(t) = \sum_n Y'_n(t)$ . The exterior normal,  $\{n_s\}$ , to the boundary of the safe region  $S$  depends on the point  $\underline{y} \in \partial D$  so as  $\underline{Y}(t)$  and  $Y'_n(t)$  are correlated in general. The processes  $\underline{Y}(t)$  and  $Y'_n(t)$  are independent when  $\partial D$  is plane, the response is Gaussian, and  $Y'_k(t)$  is unrelated to  $Y'_l(t)$  (16). The latter assumption is valid usually because  $D_i(t)$  and  $D_j(t)$  are nearly unrelated, as shown in Appendix I. When  $\underline{Y}(t)$  and  $Y'_n(t)$  are independent, the density  $f_{\underline{Y}, Y'_n}(\underline{y}, y'_n)$  is  $f_{\underline{Y}}(\underline{y}) f_{Y'_n}(y'_n)$  yielding from Eq. 3,

$$\nu = \sum_{k=1}^m \frac{\sigma_{kk}}{\sqrt{2\pi}} \left\{ \int_{\partial D'_k} d\underline{y} f_{\underline{Y}}(\underline{y}) + \int_{\partial D''_k} d\underline{y} f_{\underline{Y}}(\underline{y}) \right\} \quad (7)$$

where  $\partial D'_k$  and  $\partial D''_k$  are plane regions of  $\partial D$  for which  $y_k = -d'_k$  and  $y_k = d''_k$ , respectively. The parameter  $\sigma_{kk}$  is the standard deviation of the derivative,  $Y'_k(t)$ , of  $Y_k(t)$ .

The result in Eq. 7 can be given also in the form

$$\nu = \sum_{k=1}^m (\nu'_k P'_k + \nu''_k P''_k) \quad (8)$$

where  $P'_k$  and  $P''_k$  are the probabilities that  $-d'_k \leq Y_k(t) \leq d''_k$  for  $l \neq k$  conditioned on  $Y_k(t) = -d'_k$  and  $Y_k(t) = d''_k$ , respectively, at any time  $t$ . The parameters,

$$\nu'_k = \frac{1}{2\pi} \frac{\sigma_{kk}}{\sigma_k} \exp\left(-\frac{1}{2} \left(\frac{d'_k}{\sigma_k}\right)^2\right) \quad (9)$$

and

$$v_k'' = \frac{1}{2\pi} \frac{\sigma_{kk}}{\sigma_k} \exp\left(-\frac{1}{2} \left(\frac{d_k''}{\sigma_k}\right)^2\right) \quad (10)$$

are the mean rates at which  $Y_k(t)$  crosses from above the level  $-d_k'$  and from below the level  $d_k''$  (4,12). A knowledge of the density of  $\underline{Y}(t)$  at any time  $t$ , standard deviations of  $\{Y_k'(t)\}$ , and  $\{d_k', d_k''\}$  is needed to find  $v$ . The parameters  $v_k'$  and  $v_k''$  depend simply on the standard deviation,  $\sigma_k'$ , of  $Y_k'(t)$  and  $\sigma_{kk}$ . However, practical use of Eqs. 5 and 8 is limited due to numerical difficulties for estimation of  $P_k'$  and  $P_k''$  when  $m \geq 3$ .

A conservative approximation for the mean failure rate,  $v$ , can be obtained from Eq. 8 if the probabilities  $\{P_k'\}$  and  $\{P_k''\}$  are assumed equal to unity.

$$v \leq \tilde{v} = \sum_{k=1}^m v_k = \sum_{k=1}^m (v_k' + v_k'') \quad (11)$$

The approximate mean failure rate is attractively simple as it depends only on the standard deviations of  $\{Y_k(t)\}$  and  $\{Y_k'(t)\}$  and the design levels,  $\{d_k', d_k''\}$ . The parameter  $v_k = v_k' + v_k''$  is also the mean rate at which the  $k$ 'th critical point fails if considered separately.

Results reported in (16) and Figs. 4 to 7 show that the approximation in Eq. 11 is accurate in many cases. From (16), the approximate mean rate at which a shear frame with three degrees-of-freedom,  $d_k' = d_k'' = d$ ,  $m=n=3$ , and modal parameters given in Table 1 fails is nearly equal to  $v$ , although the response vector has strongly related components. The correlation coefficient between the interstory displacements  $Y_1(t)$  and  $Y_2(t)$  is 0.9396, for example.

Satisfactory results are reported also in Figs. 4 to 7 for square and rectangular safe regions when the Gaussian response vector,  $\underline{Y}(t)$ , has  $m=2$  components with zero mean, unit variance, and correlation coefficient  $r$ . The components of  $\underline{Y}(t)$  have unit variance and are assumed unrelated to  $\underline{Y}(t)$ . Shown in Figs. 4 and 6 is the variation of  $\tilde{v}$  and  $v$  with the level,  $d$ , for selected values of  $r$ . The ratio of exact to approximate mean failure rates is demonstrated in Figs. 5 and 7.

From Figs. 4 to 7, accurate estimates of safety can be obtained in general from the approximate mean failure rate,  $\tilde{v}$ . The approximation is most satisfactory when the components of the response vector are not strongly related. It can be too conservative when the correlation between  $\{Y_k(t)\}$  is strong and the critical points have nearly equal safety. In these cases, the mean failure rate,  $v$ , can be approximated by any  $v_k$  because the components of  $\underline{Y}(t)$  cross  $\partial D$  simultaneously. The approximate mean failure rate,  $\tilde{v}$ , is always accurate when critical points have different safety levels and safe structures are involved. Results show also that the hypothesis, that the structure

is as safe as its critical points, is unconservative. The hypothesis can be unsatisfactory in many cases.

#### RISK DEPENDENT DESIGN

Evaluation of required strength for elements of structures with known geometrical parameters and material is considered. The approach follows current design practice based on the verification of various design strategies. Modal parameters, geometrical configuration of the structure, and the frequency content of the earthquake need to be known to find the seismic response and to check adequacy of a design strategy.

#### Design Response

Current procedures for seismic design, such as the response spectrum method, are deterministic. Design levels,  $\{d_k\}$ , at any critical point,  $k$ , of a structure can be found by combining modal response maxima,  $\{d_{kj}\}$ . For example, the maximum earthquake effect at the  $k$ 'th critical point predicted by the ABS and RSS rules are, respectively,

$$d_k = \sum_{j=1}^n |d_{kj}| \quad (12)$$

and

$$d_k = \left( \sum_{j=1}^n d_{kj}^2 \right)^{1/2} \quad (13)$$

The maximum response,  $d_{kj}$ , at  $k$  in the  $j$ 'th mode of vibration is deterministic and can be obtained from the response spectrum.

Modal combination rules can be applied also when the ground acceleration,  $A(t)$ , and the modal coordinates,  $\{D_j(t)\}$ , are random. In this case, the maxima,  $\{D_{kj}\}$ , of the modal responses,  $\{c_{kj} D_j(t)\}$ , observed for a period,  $\tau$ , are also random. Application of Eqs. 12 and 13 requires the replacing of  $\{D_{kj}\}$  by related deterministic quantities,  $\{d_{kj}\}$ .

From (5, 14),  $d_{kj}$  can be assumed equal to the mean of the maximum modal response,

$$d_{kj} = \bar{D}_{kj} = c_{kj} \sqrt{\frac{\pi G_0 \Gamma_j^2}{4\beta_j \omega_j^3}} \left( \sqrt{2 \ln(\omega_j \tau)} + \frac{0.5772}{\sqrt{2 \ln(\omega_j \tau)}} \right) \quad (14)$$

because the uncertainty in  $D_{kj}$  is generally small. Modal response maxima can be approximated also by  $d_{kj} = \bar{D}_{kj} + \alpha \sigma_{k,j}$ , where  $\alpha = 1, 2, \dots$  and  $\sigma_{k,j}$  is the standard deviation of  $D_{kj}$

$$\sigma_{k,j} = c_{kj} \sqrt{\frac{\pi G_0 \Gamma_j^2}{4\beta_j \omega_j^3}} \frac{\pi}{\sqrt{12 \ln(\omega_j \tau)}} \quad (15)$$

or by the (1-p) - fractile of  $D_{kj}$  (9),

$$d_{kj} = D_{kj,p} = c_{kj} \sqrt{\frac{\pi G_0 \Gamma_j^2}{4 \beta_j \omega_j^3}} \sqrt{-2 \ln\left(-\frac{2\pi}{\omega_j \tau} \ln(1-p)\right)} \quad (16)$$

Results reported in Eqs. 14 to 16 correspond to a stationary Gaussian ground acceleration,  $A(t)$ , having constant one-sided spectral density with intensity  $G_0$ , see Appendix I and (9).

A significant limitation of the current approach for seismic design is the lack of consistency from a risk point of view. Unsafe or very safe structures are generated in many situations. The approach can be unsatisfactory for design of special structures due to the limited available experience.

A risk dependent method for seismic design can be based on the approximate mean failure in Eq. 11. The method requires a knowledge of the modal parameters of the structure, the power spectral density of the earthquake, and the target mean failure rate  $v_F$ . Structures designed according to this method fail at a mean rate,  $v$ , smaller than  $v_F$ . Results show that the actual and the target mean failure rates are nearly equal for many situations of practical interest.

Design levels,  $\{d_k\}$ , produced by the risk dependent method are based on the mean rates,  $\{v_k\}$ , at which the critical points fail rather than modal response maxima. The design condition for  $d_k = d_k^* = d_k$  is

$$v_k = \frac{1}{\pi} \frac{\sigma_{kk}}{\sigma_k} \exp\left(-\frac{1}{2} \frac{d_k^2}{\sigma_k^2}\right) \leq v_{F,k} \quad (17)$$

yielding the design level

$$d_k = \sigma_k \sqrt{-2 \ln\left(\frac{\sigma_{kk}}{\sigma_k^2} \pi v_{F,k}\right)} \quad (18)$$

where  $v_{F,k} = v_F/g(k)$  is the target mean failure rate for the  $k$ 'th critical point and  $\sum_k 1/g(k) = 1$ . The parameter  $v_{F,k}$  is  $v_F/m$  when the critical points have the same safety level, for example.

As previously mentioned, the reliability of structures designed according to the risk dependent method exceeds the target value. From Eq. 17,  $v_k = v_{F,k} = v_F/g(k)$  when the design levels in Eq. 18 are used. From Eq. 11, the mean rate,  $v$ , at which the structure fails is smaller than  $\sum_k v_k = v_F$ . The degree of conservatism depends on the correlation between the components,  $\{Y_k(t)\}$ , of the response vector,  $\underline{Y}(t)$ , and the target reliability. From Eq. 2, the dependence between  $\{Y_k(t)\}$  is controlled by the correlation between modal coordinates, and the relative magnitude and sign of the influence coefficients,  $\{c_{kj}\}$ .

The design approach in Eq. 17 may yield very conservative designs for complex structures when the correlation coefficients between responses at the critical points are nearly one. In these situations, design can be based on the conditions  $v_k \leq v_F$  ( $k=1,2,\dots,m$ ) because the structure is approximately as safe as its weakest critical point,

see Figs. 5 and 7. Such a design strategy is also demonstrated in this section.

#### Design of Shear Frames

The three stories plane shear frame analysed in Ref. 1, p. 267, is designed. Modal parameters reported in (1) are also given in Table 1. The ground acceleration,  $A(t)$ , is a stationary Gaussian white noise process with one-sided spectral density of intensity  $G_0$ .

The response vector,  $\underline{Y}(t)$ , has three components denoting inter-story displacements. The frame is safe if  $|Y_k(t)| \leq d_k$  ( $k=1,2,3$ ) during  $\tau$ , where  $\{d_k\}$  are design levels obtained from Eqs. 12, 13, or 18. The influence coefficients in Eq. 2 are  $c_{kj} = \phi_{k,j} - \phi_{k-1,j}$ , where  $\underline{\phi}'_j = \{\phi_{1,j}, \phi_{2,j}, \phi_{3,j}\}$  is the  $j$ 'th modal shape and  $\phi_{k,j}$  is the displacement at floor  $k$ .

The shape and the relative size of the safe region,  $D$ , yielded by the ABS and RSS rules are nearly unchanged for the modal response maxima predicted by Eqs. 14 to 16. They are shown in Fig. 8 in the first octant of the reference  $(\check{d}_1, \check{d}_2, \check{d}_3)$ , where  $\check{d}_k = d_k/\sigma_k$  are reduced levels. As expected from Eqs. 12 and 13, the safe region produced by the ABS rule contains that yielded by the RSS rule.

Mean failure rates,  $\{\nu_k\}$ , of separate stories for designs based on the ABS and RSS rules are shown with solid and dotted lines in Fig. 8, respectively, for various  $\check{d}_1$ . Approximate mean failure rates,  $\tilde{\nu}$ , found for the two design strategies are demonstrated also. The difference between  $\check{d}_1$  yielded by the ABS and RSS rules is accounted for but the shape and the relative size of  $D$  produced by the two strategies are assumed the same for all  $\check{d}_1$ . From (16), the approximation in Eq. 11 is accurate for this structure, although the correlation coefficient,  $r_{kl}$ , between  $Y_k(t)$  and  $Y_l(t)$  takes on the values  $r_{12} = 0.9396$ ,  $r_{13} = 0.7901$ , and  $r_{23} = 0.8504$ , see Appendix II for details. The strong correlation between responses at the critical points is not due to the modal coordinates which are nearly unrelated, see Table 1 and Fig. 1. Rather, it is caused by the dominant effect of the first mode.

As previously mentioned, safety of designs yielded by Eqs. 12 to 16 depends on the modal combination rule and the modal response maxima selected. For example, the approximate mean failure rate for designs produced by the ABS compared to RSS rule is 3 to 15 times larger and  $d_1$  increases by 50% when  $d_{kj}$  varies from  $\bar{D}_{kj}$  to  $\bar{D}_{kj} + 5\sigma_{k,j}$  or  $D_{kj,p}$  with  $p = 10^{-5}$ . These results and those in Fig. 8 demonstrate the lack of consistency from a risk point of view of the current approach for seismic design.

On the other hand, the reliability of structures designed from Eq. 18 slightly exceeds the target value for many practical situations, as reported in (16) and Figs. 4 to 7. In addition, the risk dependent design method and the design approach based on Eqs. 12 to 16 have the same level of complexity.

Designs based on Eq. 18 require a knowledge of the standard deviations,  $\{\sigma_k; \sigma_{kk}\}$ , of  $\{Y_k(t); Y'_k(t)\}$ , the target mean failure rate,  $v_F$ , and  $\{g(k)\}$ . Evaluation of  $\sigma_k$  and  $\sigma_{kk}$  is demonstrated in Appendix II. From Eq. 18 with  $g(k) = m = 3$ , the reduced design levels  $\bar{d}_1 = 3.58$ ;  $\bar{d}_2 = 3.67$ ;  $\bar{d}_3 = 3.67$  are obtained when  $v_F = 10^{-2}$ . The shape of the safe region yielded by Eq. 18 for this design situation is similar to that found from the RSS rule. However, the design level, or the size of the safe region, produced by the RSS rule is independent of  $v_F$ .

#### Design of Structures with Torsional and Translational Modes

A one-story building similar to that analysed in (11, 13) is considered, see Fig. 9. The mass is uniformly distributed on the floor but the centers of mass and stiffness are on the x-axis at a distance  $e=0.05 a$ . The structure is symmetric with respect to the x-axis so as only two modes involving translation in the y-direction and rotation about the mass center are excited when the earthquake acts as in Fig. 9. The stiffnesses in the x and y-directions are proportional to  $2b_x^3$  and  $b_y^3$ , respectively. The ground acceleration,  $A(t)$ , is as in the previous example.

Shown in Fig. 10 with dotted and solid lines are, respectively, the ratio,  $\omega_2/\omega_1$ , of modal frequencies and the correlation coefficient,  $\rho$ , between the modal coordinates as a function of  $b_y/b_x$ . The largest correlation between  $D_1(t)$  and  $D_2(t)$  is approximately 0.7. It is obtained for  $b_y/b_x = 1.4$  when the modal damping ratios are  $\beta = \beta_1 = \beta_2 = 0.10$ . The dependence of  $\omega_2/\omega_1$  and  $\rho$  on  $b_y/b_x$  is expected. For example,  $\omega_2/\omega_1$  is infinity as  $b_y$  vanishes because the structure is symmetric. Large  $\omega_2/\omega_1$  are obtained also when  $b_x$  becomes small because the torsional stiffness decreases significantly.

Design can be based on the largest stresses  $Y_1(t)$  and  $Y_2(t)$  recorded at the bottom of the walls on the x and y directions, respectively. The correlation coefficient,  $r$ , between  $Y_1(t)$  and  $Y_2(t)$  is demonstrated in Fig. 11. It varies insignificantly with  $\beta$  but strongly depends on the influence coefficients. For example,  $r$  is 0.9952 when  $b_y/b_x = 0.6$ , although the correlation coefficient,  $\rho$ , between the modal coordinates is 0.0160 for  $\beta = 0.10$ . On the other hand, the design  $b_y/b_x = 1.4$  and  $\beta = 0.10$  for which  $\rho \approx 0.70$  yields only  $r = 0.4518$ . As expected from Appendix II,  $r$  is nearly independent of  $\beta$  because the modal coordinates are not strongly related.

The risk dependent method is applied for design of structures with  $b_y/b_x = 0.6$  and 1.4 and selected mean failure rates,  $v_F = v_F \sqrt{k_y/M}$ , where  $k_y$  is the stiffness in the y direction and  $M$  is the total mass. The damping ratio assumed is  $\beta = 0.10$  for both modes. Safety conditions  $v_k = v_F$  and  $v_k = v_F/m = v_F/2$  are used when  $b_y/b_x = 0.6$  due to the strong correlation between  $Y_1(t)$  and  $Y_2(t)$ . From Table 2, the design level is less sensitive than the mean failure rate to the safety condition selected. It follows that design can be based on Eq. 18 even when the response vector has strongly related

components. The design for  $b_y/b_x = 1.4$  is based on Eq. 18 only due to the low correlation between  $Y_1(t)$  and  $Y_2(t)$ . As expected from Figs. 4 to 7, the reliability of designs produced slightly exceeds the target value.

#### CONCLUSIONS

A conservative method for seismic design yielding structures with safety levels nearly equal to the target value has been developed. Application of this risk dependent design method is relatively simple and requires a knowledge of the spectral density of the ground acceleration, the target mean failure rate, and the modal parameters of the structure.

Design is based on the condition that the critical points of a structure fail at a mean rate equal to a fraction of the target mean failure rate required for the structure. The sum of the mean failure rates for the critical points is equal in general to the target value considered for the structure. The safety conditions may differ when the response vector has strongly related components and the structure is complex. Designs yielded by the risk dependent method strongly depend on the target mean failure rate. In contrast, current approaches for seismic design based on modal response maxima cannot produce structures of prescribed reliability.

The risk dependent method has been applied for design of a plane shear frame and an asymmetrical one-story building subjected to a stationary Gaussian ground acceleration with one-sided spectral density of constant intensity. Design situations considered involve very different correlation levels between modal coordinates and between responses at the critical points. Results show that the risk dependent method is accurate for many practical situations.

#### APPENDIX I - CORRELATION BETWEEN MODAL COORDINATES

Consider a multidegree-of-freedom structure having the coordinates  $D_i(t)$  and  $D_j(t)$  for the  $i$ 'th and  $j$ 'th mode, respectively. The vector  $\underline{X}^T(t) = \{D_i(t), D_i'(t), D_j(t), D_j'(t)\}$  satisfies the linear system,

$$\underline{X}'(t) = \underline{F} \underline{X}(t) + \underline{H} A(t) \quad (19)$$

where  $A(t)$  is the ground acceleration, and

$$\underline{F} = \begin{bmatrix} 0 & 1 & 0 & 0 \\ -\omega_i^2 & -2\beta_i \omega_i & 0 & 0 \\ 0 & 0 & 0 & 1 \\ 0 & 0 & -\omega_j^2 & -2\beta_j \omega_j \end{bmatrix}, \quad \underline{H} = \begin{bmatrix} 0 \\ -\Gamma_i \\ 0 \\ -\Gamma_j \end{bmatrix} \quad (20)$$

The state  $\underline{X}(t)$  is random when  $A(t)$  is a stochastic process. As the real part,  $-\beta_i \omega_i$  or  $-\beta_j \omega_j$ , of the eigenvalues of  $\underline{F}$  is negative,

the random process,  $\underline{X}(t)$  is stationary in the wide sense when  $t$  is large and  $A(t)$  is weakly stationary (6,8,15). For large  $t$ , the mean of  $\underline{X}(t)$  is zero if the ground acceleration is a zero mean process. The covariance matrix,  $\underline{\Sigma} = \{\gamma_{rs}\}$ , of the state vector can be obtained in the steady-state motion from the algebraic equation (6, 15)

$$\underline{F} \underline{\Sigma} + \underline{\Sigma} \underline{F}' + \underline{H} (\pi G_0) \underline{H}' = \underline{0} \quad (21)$$

when  $A(t)$  is the white noise process with one-sided spectral density of intensity  $G_0$ .

From Eqs. 20 and 21, the variance of and the correlation coefficients,  $\{\rho_{rs} = \gamma_{rs} / (\gamma_{rr} \gamma_{ss})^{1/2}\}$ , between the modal coordinates and their derivatives are,

$$\begin{aligned} \gamma_{11} &= \frac{\pi G_0 \Gamma_i^2}{4 \beta_i \omega_i^3} & , & \quad \gamma_{22} = \omega_i^2 \gamma_{11} \\ \gamma_{33} &= \frac{\pi G_0 \Gamma_j^2}{4 \beta_j \omega_j^3} & , & \quad \gamma_{44} = \omega_j^2 \gamma_{33} \end{aligned} \quad (22)$$

and

$$\begin{aligned} \rho_{13} &= 8 \lambda \sqrt{\lambda \mu} (\lambda \mu + 1) \beta_j^2 / R \\ \rho_{24} &= \rho_{13} (\lambda + \mu) / (\lambda \mu + 1) \\ \rho_{14} &= -\rho_{23} = -4 \lambda \sqrt{\lambda \mu} (1 - \lambda^2) \beta_j^2 / R \end{aligned} \quad (23)$$

where

$$\begin{aligned} R &= 4 \lambda (\lambda \mu + 1) (\lambda + \mu) \beta_j^2 + (1 - \lambda^2)^2 \\ \lambda &= \omega_i / \omega_j \\ \mu &= \beta_i / \beta_j \end{aligned} \quad (24)$$

For example,  $\gamma_{11}$  is the variance of  $X_1(t) = D_i(t)$ ,  $\rho_{13}$  is the correlation coefficient between  $X_1(t) = D_i(t)$  and  $X_3(t) = D_j(t)$ , and  $\rho_{14}$  is the correlation coefficient between  $X_1(t) = D_i(t)$  and  $X_4(t) = D_j'(t)$ .

From Eq. 23,  $\rho_{14}$  is very small for current damping ratios so as  $D_i(t)$  and  $D_j'(t)$  can be assumed unrelated. For example, the largest absolute value of  $\rho_{14}$  is approximately 0.055 when  $\beta_i$  and  $\beta_j$  do not exceed 0.10.



## APPENDIX II - COVARIANCE MATRIX OF RESPONSE

From Eq. 2, the response vector is,

$$\underline{Y}(t) = \underline{C} \underline{D}(t) \quad (25)$$

where  $\underline{C} = \{c_{kj}\}$  is a matrix of influence coefficients depending on modal shapes and the response considered, and  $\underline{D}^T(t) = \{D_1(t), \dots, D_n(t)\}$  is the vector of modal coordinates.

The response vector is a random process stationary in the wide sense when the ground acceleration,  $A(t)$ , is weakly stationary, see Appendix I and Eq. 25. It has the mean zero when  $A(t)$  is zero mean. The covariance matrix of  $\underline{Y}(t)$  and its derivative,  $\underline{Y}'(t)$ , can be obtained from

$$\underline{\Sigma}_{YY} = \underline{C} \underline{\Sigma}_{DD} \underline{C}^T \quad (26)$$

$$\underline{\Sigma}_{YY'} = \underline{C} \underline{\Sigma}_{DD'} \underline{C}^T$$

$$\underline{\Sigma}_{Y'Y'} = \underline{C} \underline{\Sigma}_{D'D'} \underline{C}^T$$

where  $\underline{\Sigma}_{Z_1 Z_2} = E(\underline{Z}_1 \underline{Z}_2^T)$  is the covariance matrix of the random vectors  $\underline{Z}_1$  and  $\underline{Z}_2$  assumed to have zero mean.

For example, the variance of the  $k$ 'th components of  $\underline{Y}(t)$  and  $\underline{Y}'(t)$  are, respectively,

$$\sigma_k^2 = \sum_{j=1}^n c_{kj}^2 E\{D_j^2(t)\} + \sum_{\substack{i,j=1 \\ i \neq j}}^n c_{ki} c_{kj} E\{D_i(t) D_j(t)\} \quad (27)$$

and

$$\sigma_{kk}^2 = \sum_{j=1}^n c_{kj}^2 E\{D_j'^2(t)\} + \sum_{\substack{i,j=1 \\ i \neq j}}^n c_{ki} c_{kj} E\{D_i'(t) D_j'(t)\} \quad (28)$$

where  $E\{\}$  is the expectation operator. The correlation coefficient,  $r_{k\ell}$ , between  $Y_k(t)$  and  $Y_\ell(t)$  can be obtained from

$$r_{k\ell} \sigma_k \sigma_\ell = \sum_{j=1}^n c_{kj} c_{\ell j} E\{D_j^2(t)\} + \sum_{\substack{i,j=1 \\ i \neq j}}^n c_{ki} c_{\ell j} E\{D_i(t) D_j(t)\} \quad (29)$$

Results in Eqs. 27 to 29 can be approximated by (16),

$$\sigma_k^2 \approx \sum_{j=1}^n c_{kj}^2 \frac{\pi G \Gamma_j^2}{4\beta_j \omega_j^3} \quad (30)$$

$$\sigma_{kk}^2 \approx \sum_{j=1}^n c_{kj}^2 \frac{\pi G_o \Gamma_j^2}{4 \beta_j \omega_j} \quad (31)$$

$$r_{k\ell} \sigma_k \sigma_\ell \approx \sum_{j=1}^n c_{kj} c_{\ell j} \frac{\pi G_o \Gamma_j^2}{4 \beta_j \omega_j} \quad (32)$$

when the modal coordinates are nearly unrelated and the ground acceleration,  $A(t)$ , is white with one-sided spectral density of intensity  $G_o$ .

From Table 1 and Fig. 1, the modal coordinates of the three degree-of-freedom shear frame considered are nearly unrelated so as Eqs. 30 to 32 can be applied to find the covariance matrix of  $\underline{Y}(t)$  and  $\{\sigma_{kk}\}$ . The following results are obtained when the components of  $\underline{Y}(t)$  are interstory displacements, also see (16),

$$\sigma_1^2 = 0.203 \frac{G_o}{32\pi^2\beta} \quad ; \quad \sigma_2^2 = 0.280 \frac{G_o}{32\pi^2\beta} \quad ; \quad \sigma_3^2 = 0.250 \frac{G_o}{32\pi^2\beta} \quad (33)$$

$$\sigma_{11}^2 = 0.0317 \frac{G_o}{\beta} \quad ; \quad \sigma_{22}^2 = 0.0448 \frac{G_o}{\beta} \quad ; \quad \sigma_{33}^2 = 0.0598 \frac{G_o}{\beta} \quad (34)$$

and

$$r_{12} = 0.9396; \quad r_{13} = 0.7901; \quad r_{23} = 0.8504 \quad (35)$$

when the damping ratio is the same for all modes,  $\beta_j = \beta$ , and  $A(t)$  is the white process previously considered. From Eqs. 23 and 26 and Table 1, the correlation coefficients between  $Y_k(t)$  and  $Y_\ell(t)$  are nearly zero so as Eq. 7 can be applied.

#### APPENDIX III - REFERENCES

1. Biggs, M., Introduction to Structural Dynamics, McGraw-Hill Book Co., New York, 1964.
2. Bolotin, V.V., Primenenie Metodov Teorii Veroiatnostei i Teorii Nadejnosti v Raschetak Soorujenii, Izdatelstvo Literaturi po Stroitelstvu, Moskov, 1967.
3. Cornell, C.A., "Bounds on the Reliability of Structural Systems", Journal of Structural Division, ASCE, Vol. 93, No. ST1, Proc. Paper 5096, February, 1967, p. 171-200.
4. Cramer, H. and Leadbetter, M.R., Stationary and Related Stochastic Processes, John Miley & Sons, New York, 1967.
5. Davenport, A.G., "Note on the Distribution of the Largest Value of a Random Function with Application to Gust Loading", Proceedings, Institute of Civil Engineers, London, Vol. 28, 1964, pp. 187 - 196.

6. Gelb, A., ed., Applied Optimal Estimation, The Massachusetts Institute of Technology Press, Cambridge, Massachusetts, 1974.
7. Grigoriu, M. and Turkstra, C., "Safety of Structural with Correlated Resistances", Structural Mechanics Series, No. 78-1, McGill University, Department of Civil Engineering, Montreal, Canada, Jan. 1978, approved for publication to Applied Mathematical Modelling, England.
8. Grigoriu, M., "Prediction and Simulation with Auto-regressive Models in Hydrology", presented at the May 22-24, 1978, Chapman Conference on Applications of Kalman Filtering Theory and Technique, held at Pittsburgh, Pennsylvania, U.S.A.
9. Grigoriu, M., "Extremes of Moving Average Processes", presented at the Jan. 29 - Feb. 2, 1979, Applications of Statistics and Probability in Soil and Structural Engineering, held at Sydney, Australia.
10. Hasofer, A.M., "The Upcrossing Rate of a Class of Stochastic Processes", Studies in Probability and Statistics, (papers in honour of E.J.G. Pitman), edited by E.J. Williams, Jerusalem Academic Press, 1974, pp. 153-160.
11. Newmark, N.M. and Rosenblueth, E., Fundamentals of Earthquake Engineering, Prentice-Hall Inc., Englewood Cliffs, N.J., 1971.
12. Rice, S.O., "Mathematical Analysis of Random Noise", Bell System Technical Journal, Vol. 24, 1945, pp. 46-156.
13. Rosenblueth, E., and Elorday, J., "Responses of Linear Systems to Certain Transient Disturbances", Proceedings of the Fourth World Conference on Earthquake Engineering, Chilean Association on Seismology and Earthquake Engineering, Vol. 1, Jan. 1969, pp. 185-196.
14. Ruiz, P., "On the Maximum Response of Structures Subjected to Earthquake Excitations", Proceedings of the Symposium on Earthquake Engineering, University of Roorkee, 1970, pp. 272-277.
15. Schweppe, F.C., Uncertain Dynamic Systems, Prentice-Hall Inc., Englewood Cliffs, New Jersey, 1973.
16. Veneziano, D., Grigoriu, M., and Cornell, C.A., "Vector-Process Models for System Reliability", Journal of the Engineering Mechanics Division, ASCE, Vol. 103, No. EM3, Proc. Paper 12981, June, 1977, pp. 441-460.

TABLE 1

Modal Parameters of the Shear Frame (from Ref.1, p.267)

Modal Parameters (1)	Mode j		
	1 (2)	2 (3)	3 (4)
$\omega_j / (2\pi)$	1.00	2.18	3.18
$\Phi_{j,1}$	0.314	-0.511	3.18
$\Phi_{j,2}$	0.685	-0.489	-2.18
$\Phi_{j,3}$	1.00	1.00	1.00
$\Gamma_j$	1.40	-0.50	0.098

TABLE 2

Risk Dependent Design. The Case  
 $b_y/b_x = 0.60$ ;  $r_{12} = 0.9952$ ;  $\beta = 0.10$

$v_F^*$ (1)	$v/v_F$		$\tilde{d}_1$		$\tilde{d}_2$	
	$v_k = v_F/2$ (2)	$v_k = v_F$ (3)	$v_k = v_F/2$ (4)	$v_k = v_F$ (5)	$v_k = v_F/2$ (6)	$v_k = v_F$ (7)
$10^{-5}$	0.59	1.17	4.72(3%)	4.58	4.70(3%)	4.55
$10^{-4}$	0.58	1.15	4.21(4%)	4.04	4.19(4%)	4.02
$10^{-3}$	0.57	1.13	3.62(6%)	3.42	3.59(6%)	3.39
$10^{-2}$	0.56	1.10	2.92(9%)	2.67	2.88(10%)	2.63

TABLE 3

Risk Dependent Design. The Case  
 $b_y/b_x = 1.40$ ;  $r_{12} = 0.4518$ ;  $\beta = 0.10$

$v_F^*$ (1)	$v/v_F$ (2)	$\bar{d}_1$ (3)	$\bar{d}_2$ (4)
$10^{-5}$	0.9981	4.7026	4.6997
$10^{-4}$	0.9949	4.1844	4.1812
$10^{-3}$	0.9863	3.5922	3.5884
$10^{-2}$	0.9614	2.8807	2.8761

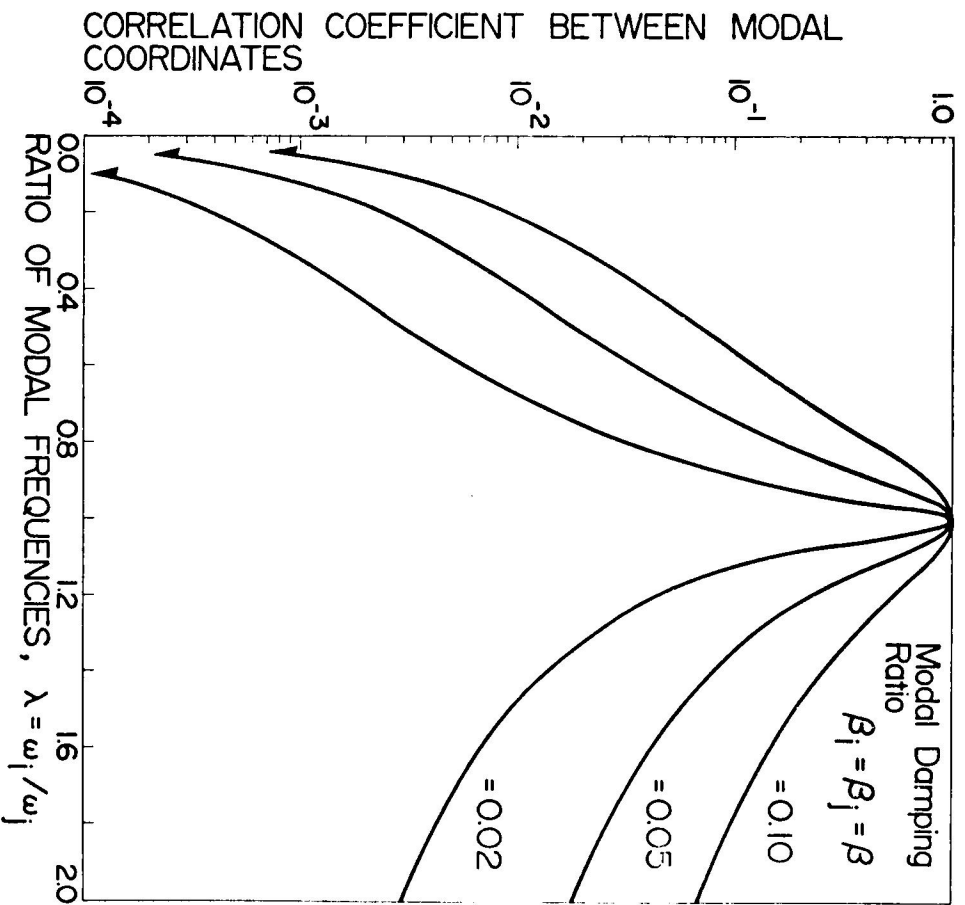


Fig. 1 - Dependence of correlation between modal coordinates on ratio of modal frequencies. The case  $\beta_i = \beta_j$ .

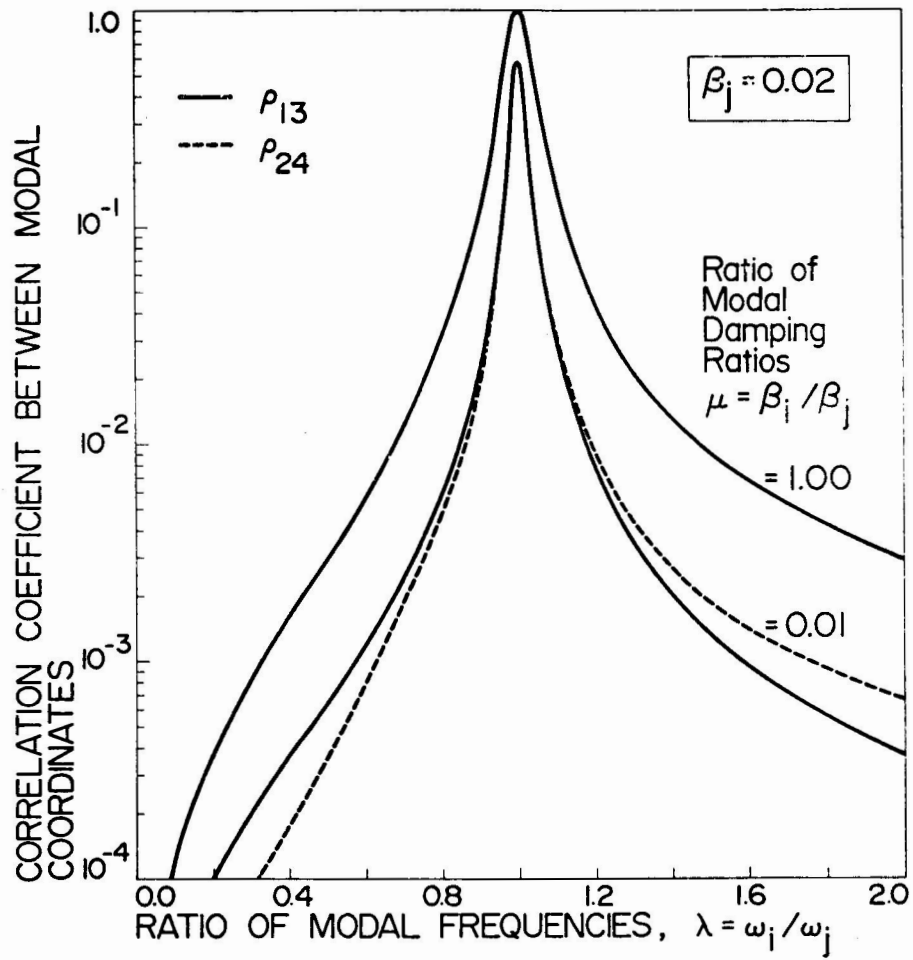


Fig. 2 - Dependence of correlation between modal coordinates on ratio of modal frequencies.

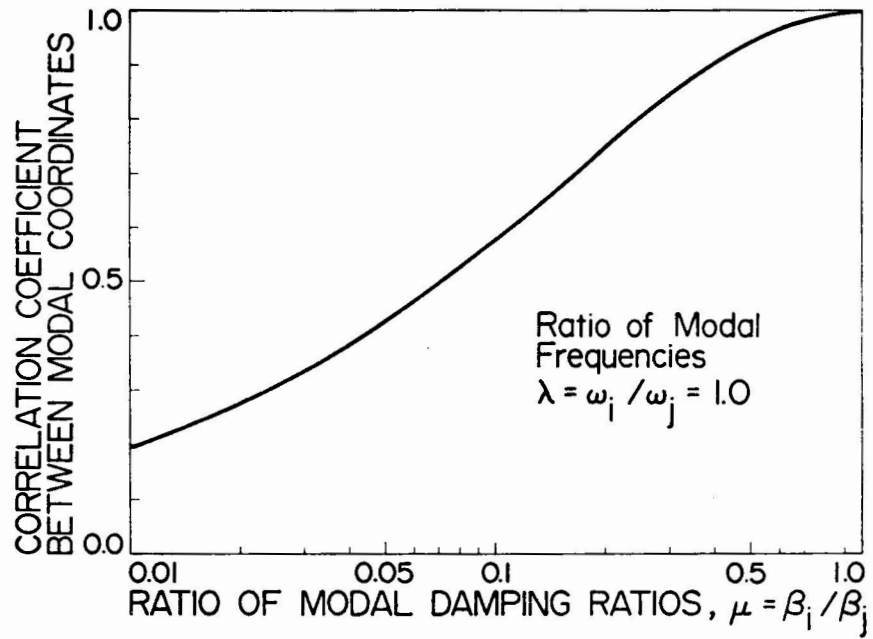


Fig. 3 - Dependence of correlation between modal coordinates on ratio of modal damping coefficients. The case  $\omega_i = \omega_j$ .



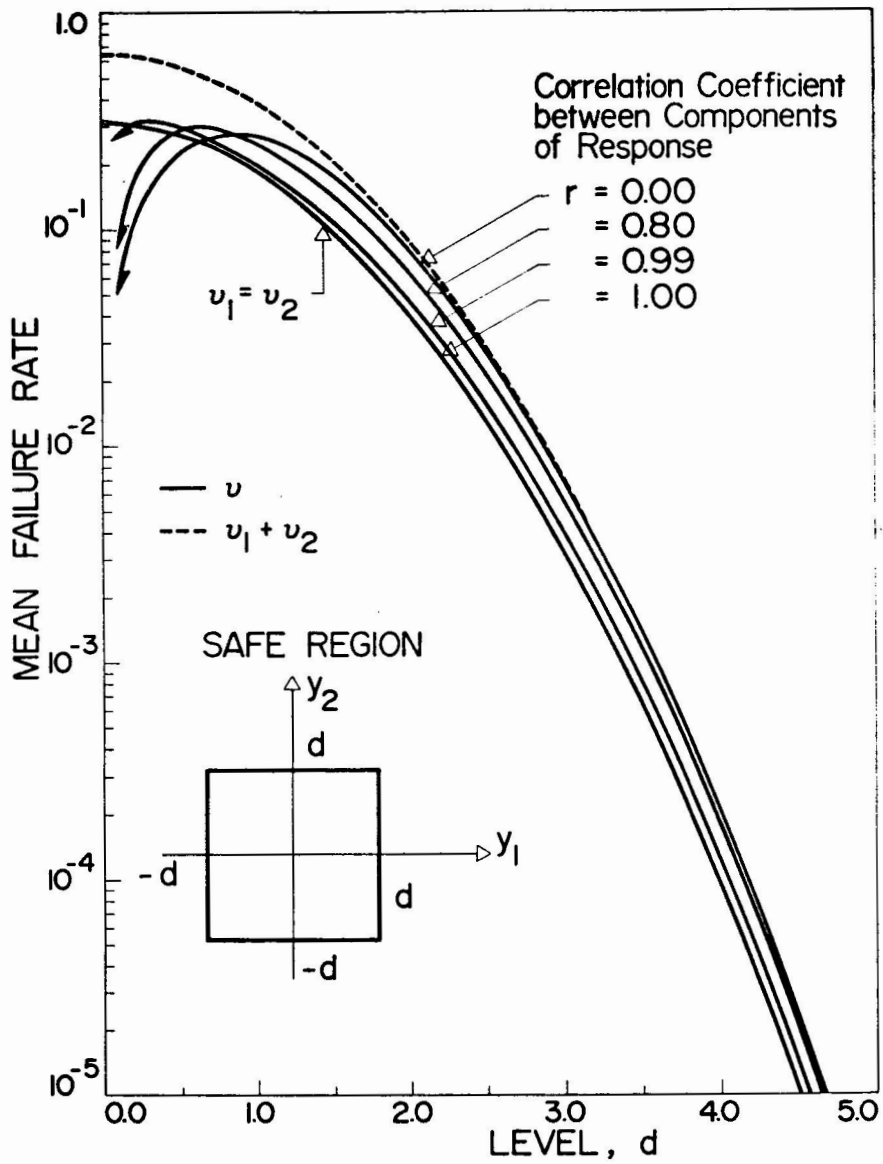


Fig. 4 - Dependence of mean failure rate on correlation between components of response for square safe regions.

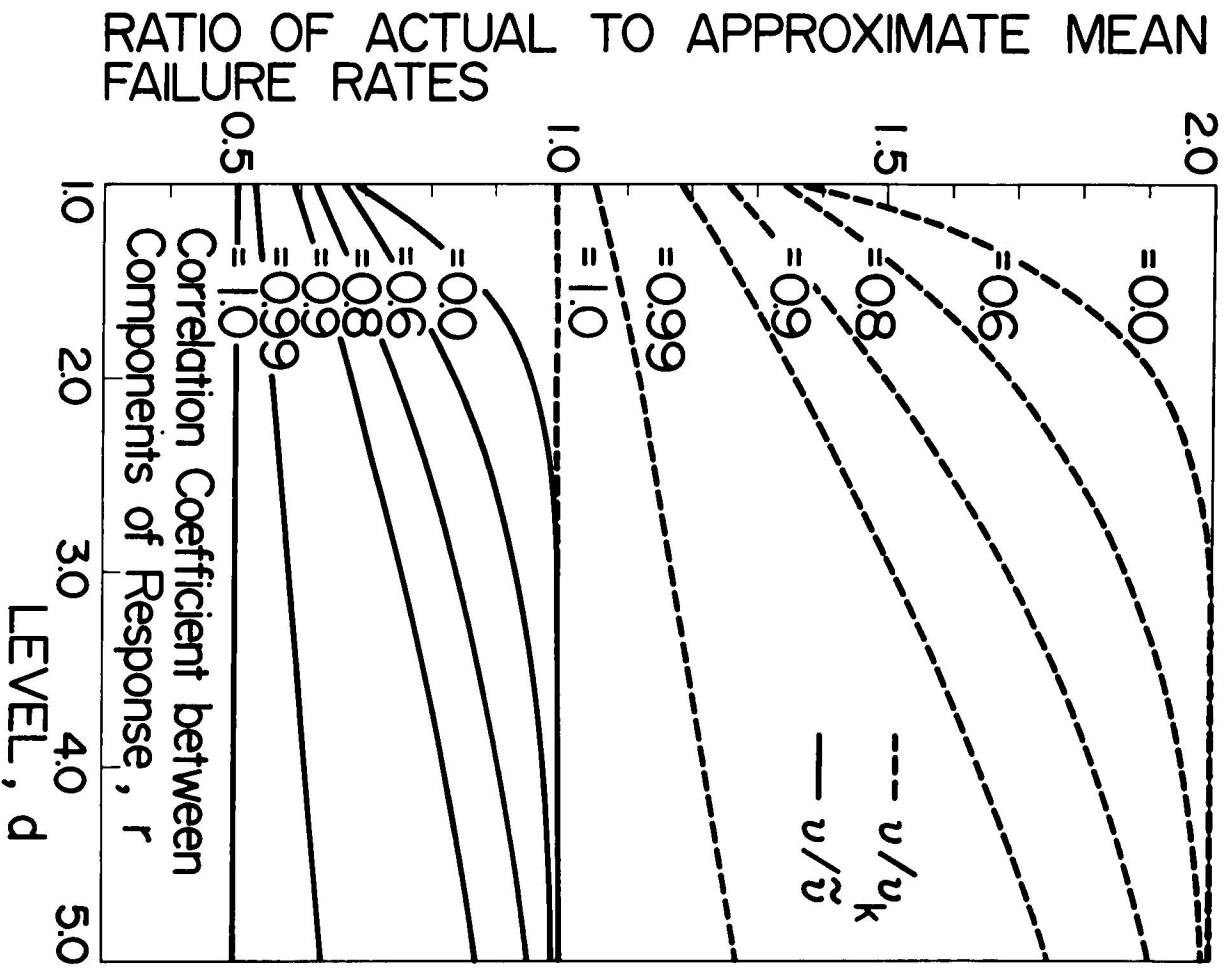


Fig. 5 - Ratio of exact to approximate mean failure rates for square safe regions.

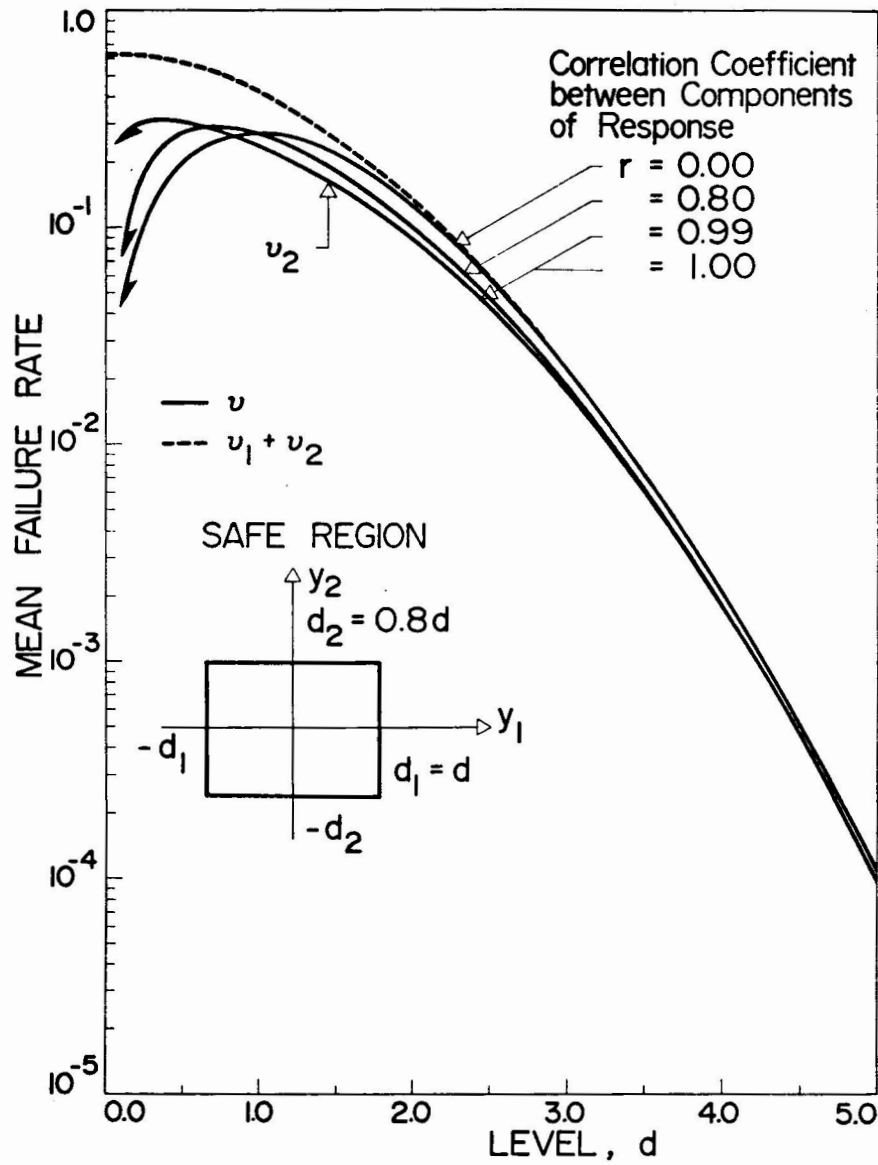


Fig. 6 - Dependence of mean failure rate on correlation between components of response for rectangular safe regions.

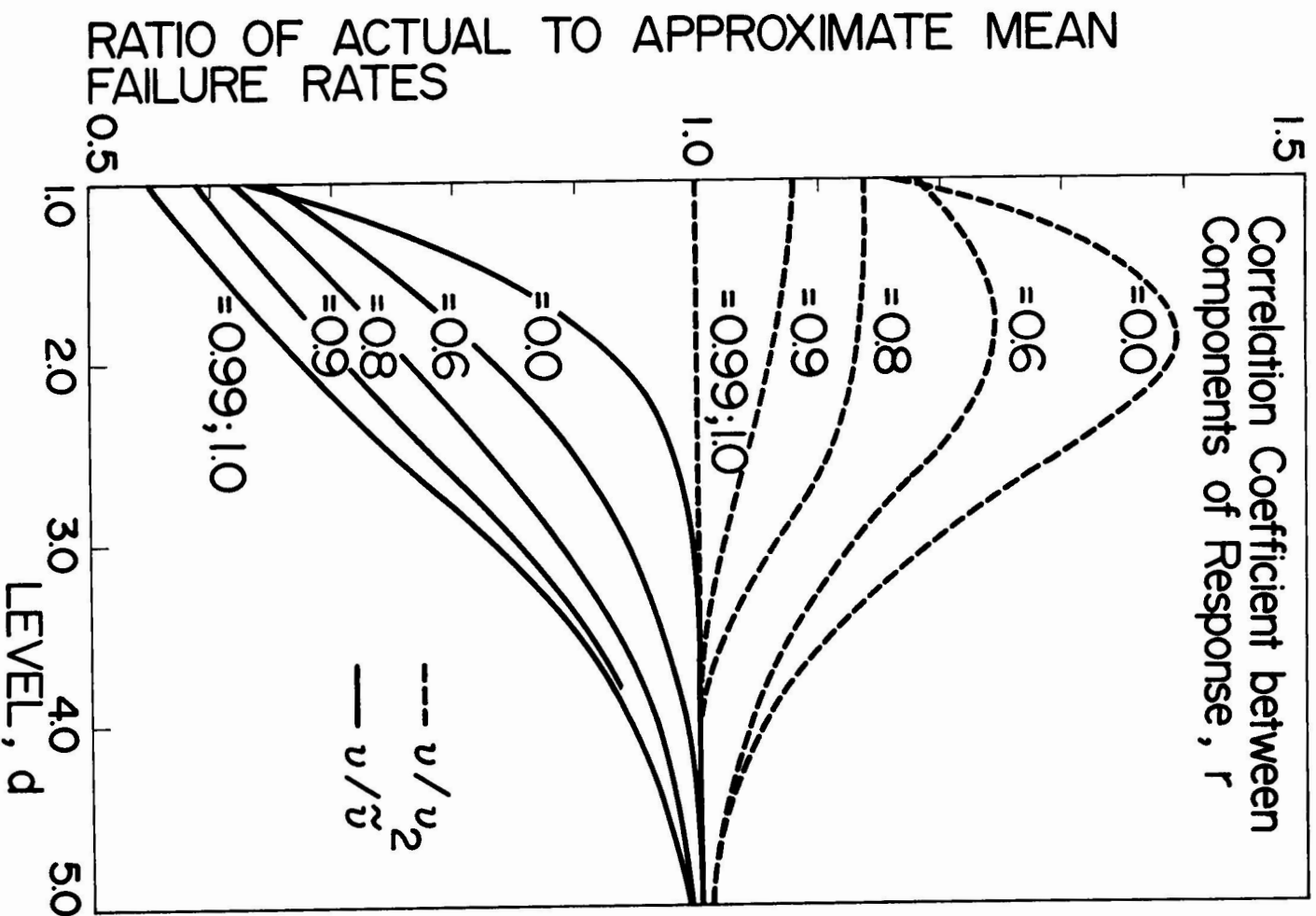


Fig. 7 - Ratio of exact to approximate mean failure rates for rectangular safe regions.

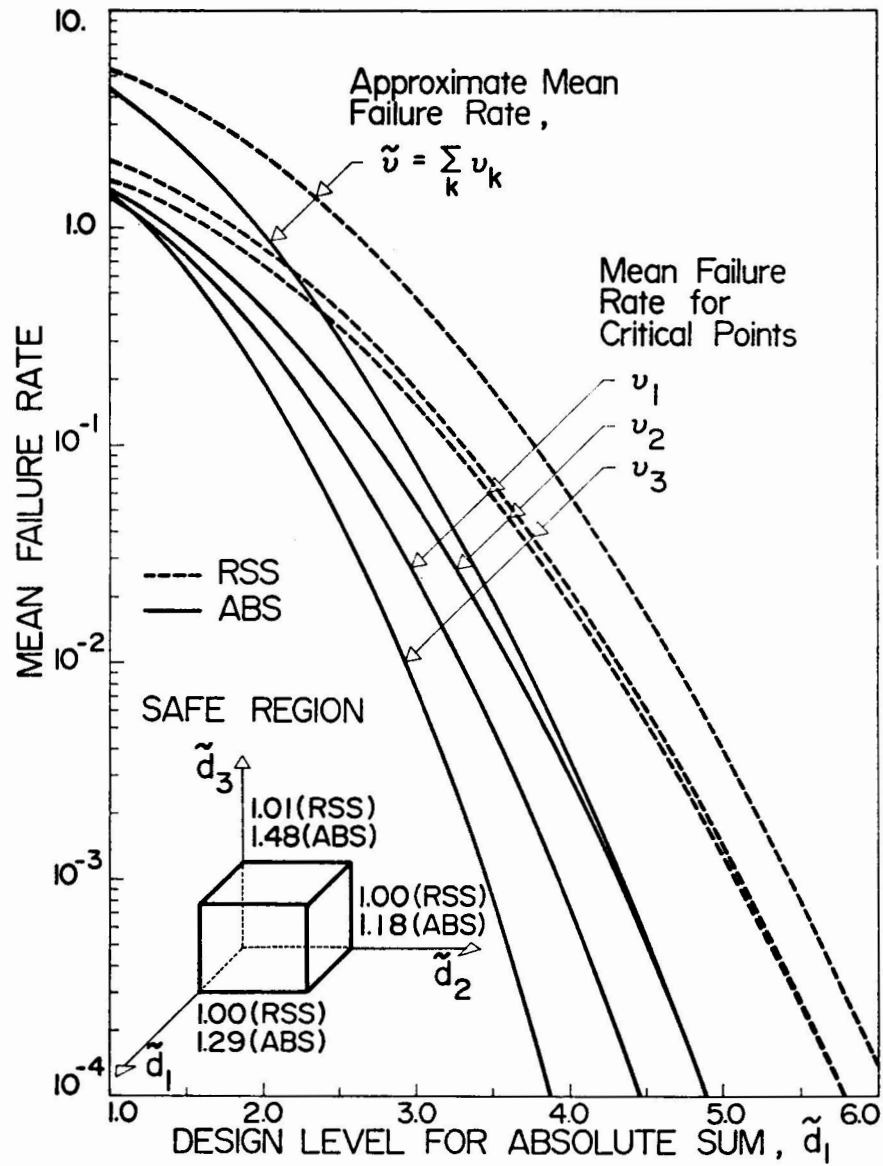


Fig. 8 - Mean failure rates for designs yielded by the ABS and RSS rules.

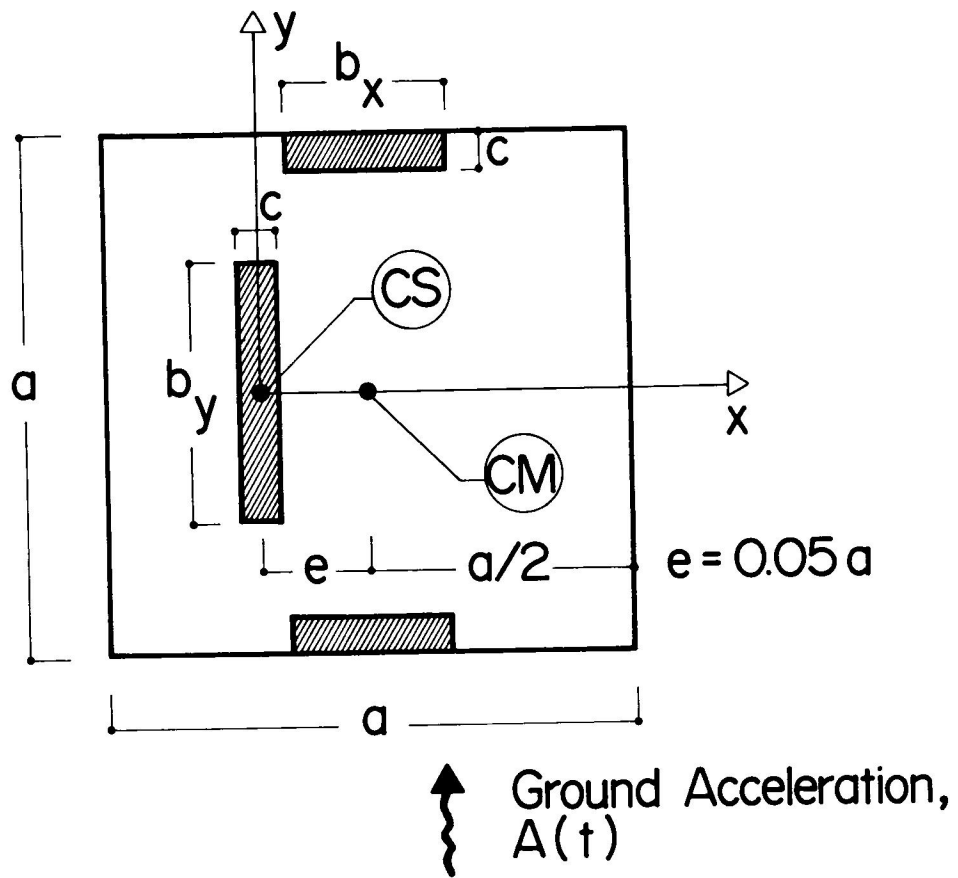


Fig. 9 - Asymmetrical structure subjected to earthquake.

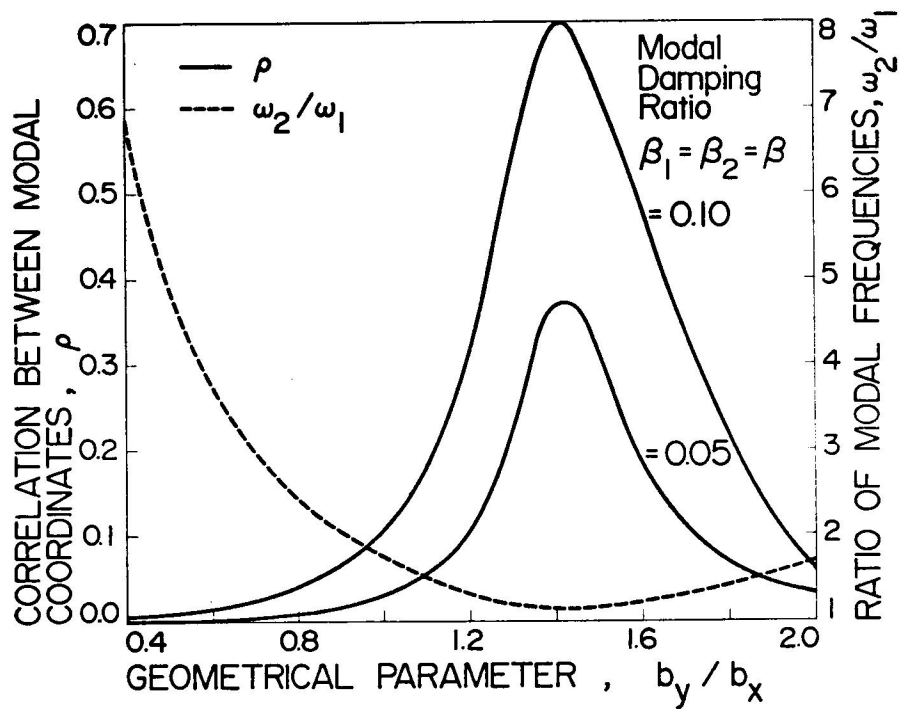


Fig. 10 - Correlation between modal coordinates for the structure in Fig. 9.

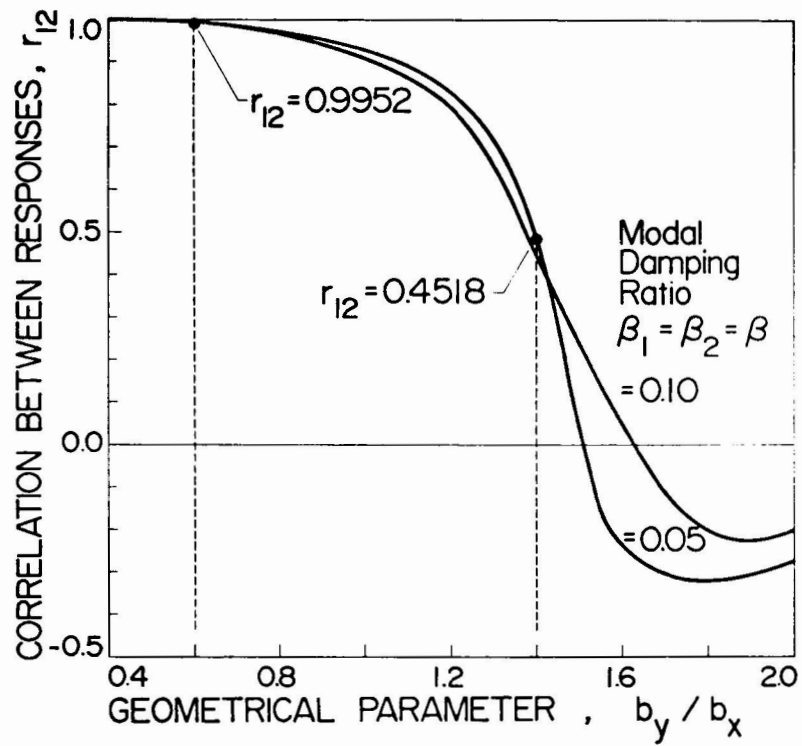


Fig. 11 - Correlation between responses at critical points for the structure in Fig. 9.